Enhanced Solubility and Bioavailability of Scutellarin via Amorphous Nanoparticles Stabilized with PVP

Xin Cheng[a1] https://orcid.org/0000-0003-3794-8519, Qin Lv[a1], Shuang Tian[a] https://orcid.org/0009-0005-8485-7531, Guiyan Jin[a], Wenbin Jin[a], Jiao Wang[a*], Wenping Wang[a,b*] https://orcid.org/0009-0009-6115-3880

[a] College of Chinese Materia Medica, Yunnan University of Chinese Medicine, Kunming 650500, China

[b] Key Laboratory of Yunnan Provincial Department of Education for Processing Research on Characteristic Prepared Drug in Pieces. Kunming 650500, China.

[1] They contributed equally to this work.

[*] Corresponding authors.

E-mail addresses: wangwenping@ynucm.edu.cn (W.W.); 1750482115@qq.com (J.W .).

Telephone numbers: +-86-87167495503 (W.W.);

Submitted 2025/9/27
Revised 2025/2/26
Accepted 2026/3/26

Abstract

Purpose: Scutellarin (SCU) is a bioactive flavonoid whose therapeutic applications are limited by its poor aqueous solubility and low bioavailability. This study aimed to develop amorphous SCU nanoparticles stabilized with polyvinyl pyrrolidone K30 (PVP) via an anti-solvent precipitation method to enhance solubility, dissolution, and oral bioavailability.

Methods: Amorphous SCU-PVP nanoparticles were prepared by ultrasonically dispersing SCU solution in dimethyl sulfoxide into dichloromethane containing PVP (solvent: anti-solvent ratio 1:40; SCU:PVP 1:1 w/w). The nanoparticles were characterized in terms of morphology (SEM), particle size (DLS), crystallinity (DSC, PXRD), drug-polymer interactions (FTIR), drug loading, solubility, and *in vitro* dissolution. Pharmacokinetics were evaluated in male

Sprague-Dawley rats orally administered 100 mg/kg SCU as nanoparticles or bulk SCU. Plasma drug concentrations were quantified via HPLC, and parameters were analyzed using DAS 3.2.1.

Results: The optimized nanoparticles exhibited an average size of 150 nm (pre-drying) and 800 nm (post-drying), with high drug loading (40%) and encapsulation efficiency (85%). FTIR and Hansen parameter calculations ($\Delta\delta_t$= 8.18, R_a= 17.64) confirmed hydrogen bonding and miscibility between SCU and PVP. Amorphization (via DSC/PXRD) enhanced SCU solubility 5.8-fold in water. *in vitro* dissolution studies showed >80% SCU release within 5 min across all pH media (vs. <3% for bulk drug). Pharmacokinetic studies revealed 130% relative oral bioavailability and prolonged $T_{1/2}$ for nanoparticles versus bulk SCU.

Conclusion: PVP-stabilized amorphous nanoparticles significantly improve SCU's solubility, dissolution rate, and oral bioavailability via hydrogen bonding and amorphization. This simple, scalable anti-solvent precipitation method offers a promising strategy for enhancing the delivery of poorly soluble flavonoids.

Keywords: scutellarin, nanoparticle formulation, amorphous state, PVP stabilization, solubility enhancement, supramolecular interactions

1. Introduction

Flavonoids, a class of hydroxylated phenolic compounds, have attracted considerable research interest due to their diverse health benefits.[1] However, most flavonoids exhibit poor water solubility, low bioavailability, and rapid metabolism *in vivo*, which limit their clinical application.[2] Nanotechnology offers a promising approach to overcoming these limitations, enhancing drug solubility and delivery efficiency.[3] Nanoparticles, in particular, provide significant advantages for pharmaceutical formulations, such as improved stability and targeting capabilities.[4,5]

Various synthetic polymers, natural polysaccharides, and proteins have been utilized as carriers for drug incorporation, facilitating the creation of drug-loaded nanoparticles through self-assembly or crosslinking.[6,7] Scutellarin (SCU), a flavone glycoside derived from the Chinese medicinal herb *Erigeron breviscapus*, possesses a wide range of pharmacological

effects, including anti-inflammatory, antioxidant, and neuroprotective properties.[8–10] SCU has been widely used for the treatment of cardiovascular and cerebrovascular diseases. However, improving its therapeutic delivery through nanotechnology remains challenging, as methods such as nanosuspensions and nanoparticle formulations need to balance high drug loading with scalable production.[11–16]

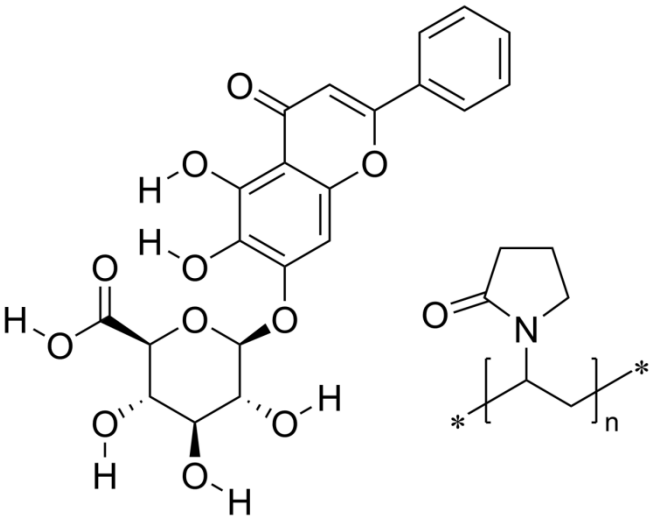

Figure 1. Chemical structures of scutellarin (left) and PVP (right).

Polyvinyl pyrrolidone (PVP) is widely used in pharmaceutical applications due to its biocompatibility and solubility in both water and various organic solvents.[17,18] PVP is available in different grades according to its K value, with K30 being particularly suitable for drug delivery systems.[19] PVP has been successfully employed to enhance the solubility and bioavailability of poorly soluble drugs, due to its ability to prevent recrystallization and stabilize amorphous dispersions.[20] Previous research has used PVP K30 to enhance dissolution of SCU and bioavailability in solid dispersion tablets.[21]

In this study, we developed amorphous SCU nanoparticles stabilized with PVP K30 using an anti-solvent precipitation method. We further analyzed drug-polymer interactions through miscibility calculations ,compared the solubility, dissolution, and pharmacokinetic profiles of SCU-PVP nanoparticles with those of unencapsulated SCU to explore the potential advantages of this formulation.

2. Materials and Methods

2.1 Materials

Scutellarin (purity > 97%) was purchased from Jingzhu Biotech Co., Ltd. (Nanjing, China). Polyvinyl pyrrolidone K30 (PVP) was sourced from Aladdin Biotech Co., Ltd. (Shanghai, China). Dimethyl sulfoxide (DMSO) and dichloromethane (DCM) ,both of analytical grade, were obtained from Tianjin Zhiyuan Chemical Reagent Co., Ltd. and Tianjin Fengchuan Chemical Reagent Technology Co., Ltd., respectively. Methanol (HPLC-grade) was supplied by Sigma-Aldrich. Ultra-purified water was prepared using an Arium® Comfort system (Sartorius, Germany) and used throughout the study.

Male Sprague-Dawley (SD) rats weighing 230± 30 g were obtained from SPF (Beijing) Biotechnology Co., Ltd. The animal study protocol was approved by the Experimental Anim al Ethics Committee of Yunnan University of Chinese Medicine(YNUTCM-XMSS-G-202500 1),with all procedures adhered to the Guidelines for the Care and Use of Laboratory Animals. The rats were fasted overnight with access to water before the experiments.

2.2 Preparation of Drug Nanoparticles

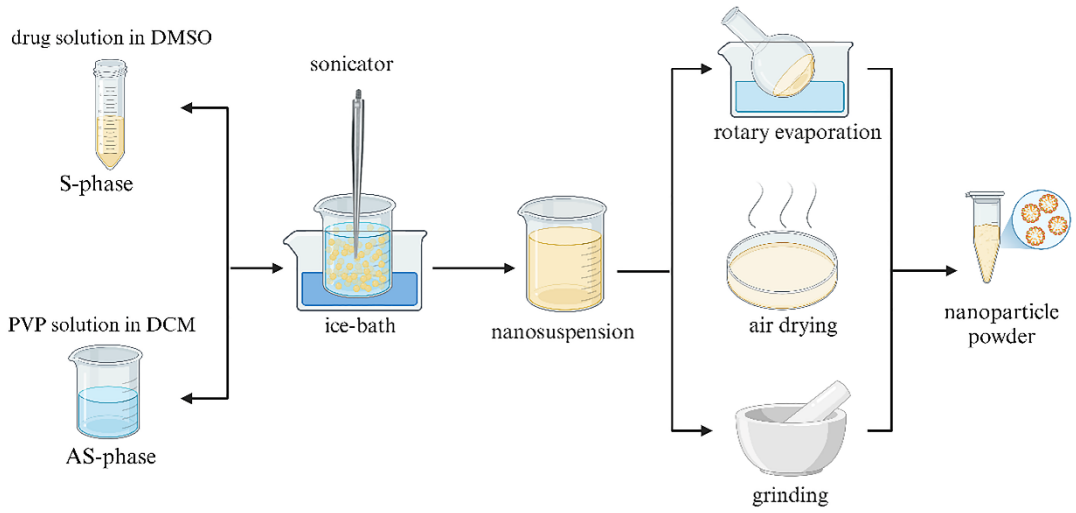

Figure 2. Flow chart illustrating the scutellarin nanosuspension and nanoparticle fabrication process.

The preparation process of SCU nanoparticles is illustrated in **Figure 2**. SCU nanosuspensions were prepared via a simple anti-solvent precipitation technique.[22] Initially,

SCU was completely dissolved in dimethyl sulfoxide (DMSO) to form the solvent phase (S-phase) at a concentration of 400 mg/mL (w/v). Concurrently, PVP was dissolved in dichloromethane (DCM) to form the anti-solvent phase (AS-phase). The S-phase was dispersed into the AS-phase at a volumetric ratio of 1:40 under ice bath conditions, using a probe sonicator set to 240 W for 1 minute, with 5-second bursts and 5-second pauses.

SCU nanoparticles were obtained by removing the solvent from the nanosuspension.[23] Approximately 80% of the organic solvent was recovered using rotary evaporation at 40°C under vacuum. The remaining suspension was transferred to a glass dish, left in a fume hood for 48 hours, and then dried at 70°C for 4 hours in an air oven. The resulting powder was ground and passed through a 100-mesh sieve before being stored in airtight containers for analysis. For comparison, additional SCU suspensions were prepared using the same method , with and without PVP.

2.3 Morphology Observation

The morphology of the raw SCU material, nanosuspensions, and nanoparticles was initially evaluated visually. The samples were suspended in water and ultrasonicated for 5 minutes to ensure uniform dispersion. Freshly prepared or redispersed suspensions were placed on microscope slides and examined under an XDS 200-PH microscope (Phenix, China). For scanning electron microscopy (SEM) analysis, the samples were sputter-coated with gold and examined using a Phenom Pro SEM (Phenom World, Netherlands) for detailed microstructural examination.

2.4 Particle Size Analysis

Particle size and polydispersity index (PDI) were determined using a NanoBrook 90 Plus dynamic light scattering (DLS) analyzer (Brookhaven Instruments, NY, USA). SCU nanosuspensions were diluted to 3 mg/mL with DCM, while nanoparticle powders were redispersed in water and ultrasonicated before analysis. Measurements were conducted in triplicate at 25°C with a detecion angle of 90° and a wavelength of 633 nm.

2.5 Solid State Characterization

The thermal properties of SCU, PVP, their physical mixtures, and nanoparticle powders were examined using differential scanning calorimetry (DSC) (X'pert PRO, Spectris, Holland). Samples were sealed in aluminum pans with perforated lids and heated from -80°C to 500°C at a rate of 10°C/min under a nitrogen atmosphere, with aluminum oxide (Al_2O_3) as the reference.

Powder X-ray diffraction (PXRD) was performed to evaluate the crystallinity of SCU in the samples using a D8 Advance diffractometer (Bruker, UK) with Cu-Kα radiation. Scans were conducted over a 2θ range of 5° to 60° at a scan rate of 8°/min.

Fourier-transform infrared (FTIR) spectra were recorded using a TENSOR37 FTIR spectrophotometer (Bruker, Germany) over a range of 400–4000 cm^{-1}. Samples were prepared by mixing with potassium bromide (KBr) and pressing the mixture into disks with a diameter of 10 mm at 10 MPa.

2.6 Compatibility Calculation

The compatibility of SCU with PVP was assessed by calculating the partial and total Hansen solubility parameters (HSP) using SMILES data entered into HSPiP software (Version 5.1.03). The differences in total HSPs ($\Delta\delta t$, $\Delta\bar{\delta}$), the volume-dependent solubility parameter (δv), and the distance in Hansen space (Ra) were calculated following previously established methods.[24]

2.7 Drug Content Determination

Accurately weighed samples were dissolved in 10 mL of methanol, filtered through a 0.22 μm syringe filter, and analyzed using HPLC. The HPLC system (Chrome UHPLC S6000, China) was equipped with an Agilent Eclipse XDB-C18 column (5 μm, 4.6 x 250 mm, Agilent, Santa Clara, CA, USA). The mobile phase consisted of methanol and 0.05% formic acid solution (65:35, v/v) at a flow rate of 0.5 mL/min, with detection at 335 nm and the column temperature maintained at 25°C. Drug loading (DL) and encapsulation efficiency (EE) were calculated as follows:

DL (%) = amount of SCU loaded / total mass × 100%

EE (%) = amount of SCU loaded / amount of SCU added × 100%

2.8 Saturated Solubility of SCU

The equilibrium solubility of SCU was measured in water and PVP solutions. Samples were equilibrated at 37°C for 72 hours in an oscillating gas bath. The supernatant was diluted with methanol, filtered, and analyzed via HPLC.

2.9 Drug Dissolution Test

Powder samples were tested for dissolution in 250 mL of water or phosphate-buffered solutions (PBS) at various pH levels. Dissolution testing was performed using a DF-101S magnetic stirrer (Gongyi Maihua Instrument Co., Ltd., China). The medium was stirred at 50 rpm and maintained at 37°C ± 0.5°C. Aliquots were taken at specific intervals, and drug concentration was determined via HPLC.

The similarity factor (f_2) was calculated using the following equation: $f_2 = 50 \times \log\{[1 + (1/n)\Sigma(R_t - T_t)^2]^{-0.5} \times 100\}$, where R_t and T_t represent the mean percentage dissolved of the reference (bulk SCU or physical mixture) and test (nanoparticle) products at each time point, respectively.[25] An f_2 value between 50 and100 indicates similar dissolution profiles.

2.10 *I*n vivo Oral Pharmacokinetic Study

An *in vivo* pharmacokinetic study was conducted to compare the oral absorption of SCU-PVP nanoparticles with that of bulk SCU in rats. Twelve Sprague-Dawley (SD) rats were randomly divided into two groups (n=6 per group). Each group was administered a single oral dose of either SCU-PVP nanoparticles or bulk SCU at 100 mg/kg through oral gavage. Blood samples (0.3 mL) were collected at predetermined time intervals (0.25, 0.5, 1, 2, 4, 6, 8, and 12 hours) after dosing. The plasma was separated by centrifugation at 4°C and 5000 rpm for 10 minutes, and then stored at -80°C until analysis.

For drug quantification, 100 µL of plasma was mixed with 100 µL of an internal standard solution (rutin, 8 µg/mL in methanol) and 100 µL of methanol, followed by centrifugation at 12,000 rpm for 10 minutes. The supernatant was filtered through a 0.1 µm syringe filter, and a 20 µL aliquot was injected into the HPLC system for drug concentration analysis, following the

same chromatographic conditions as described earlier.

The pharmacokinetic parameters, including the maximum plasma concentration (C_{max}), time to reach maximum concentration (T_{max}), area under the plasma concentration-time curve (AUC), half-life ($T_{1/2}$), and mean residence time (MRT_{0-t}), were calculated using DAS 3.2.1 software. The results were statistically analyzed using SPSS 17.0 software, and a P-value of less than 0.05 was considered statistically significant.

3. Results and Discussion

3.1 Optimization and Preparation of SCU Nanoparticles

The preparation of SCU-PVP nanoparticles involved an anti-solvent precipitation method optimized to produce a nanosuspension before drying. This approach was selected due to its efficiency in generating nanoparticles with desirable morphological characteristics.

DMSO was chosen as the solvent for SCU, in which the drug exhibited a solubility greater than 0.4 g/mL.[26] DCM was selected as the anti-solvent, as SCU's solubility in DCM is low, which facilitated the formation of well-dispersed and stable nanoparticles (see **Figures S1** and **S2**). The compatibility of polymeric stabilizers with both DMSO and DCM was also a critical consideration.

Several polymers were tested for their ability to stabilize the drug suspension, and PVP produced the finest particles and minimal aggregation after 24 hours (**Figure S3**). In contrast, Poloxamer and PEG resulted in larger and less stable particles prone to rapid sedimentation. Scanning electron microscopy (SEM) confirmed that PVP alone provided effective stabilization, preventing aggregation and ensuring a more uniform particle size distribution (**Figure S4**).

Various dispersion techniques were evaluated, and ultrasonication yielding the smallest particle sizes and ensuring a stable suspension without significant sedimentation (**Figures S5** and **S6**). The optimal S-phase to AS-phase volumetric ratio and SCU to PVP weight ratio were determined to be 1:40 and 1:1, respectively, based on particle morphology and drug loading

efficiency (**Figure S7** and **Figure 3**).

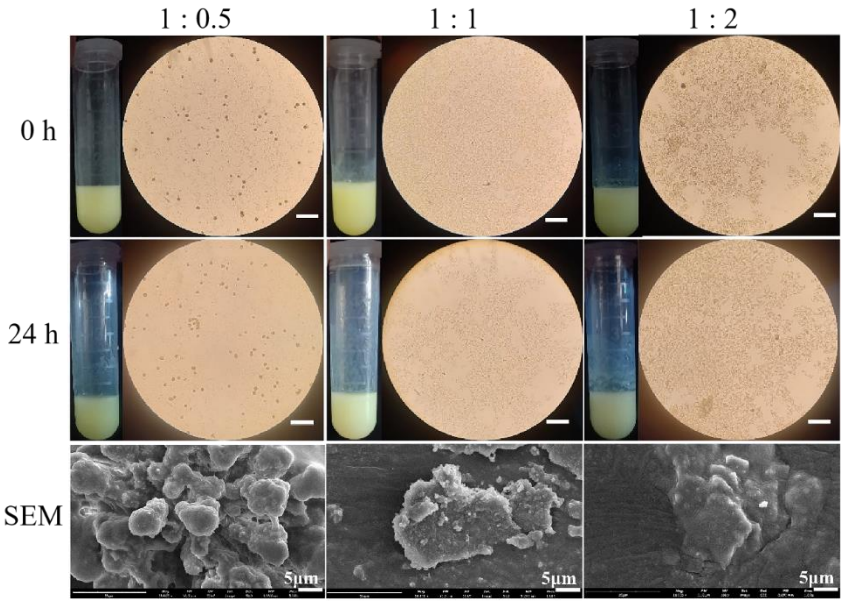

Figure 3. Appearance and micromorphology of SCU suspensions at various weight ratios of scutellarin and PVP K30 (bar size 50 μm).

In summary, this optimized protocol was straightforward and avoiding costly excipients and complex equipment. The use of DCM rather than aqueous anti-solvents improved particle dispersion and reduced processing time. The SCU-PVP nanoparticles were further evaluated in subsequent analyses.

3.2 Morphology Observation and Particle Size Analysis

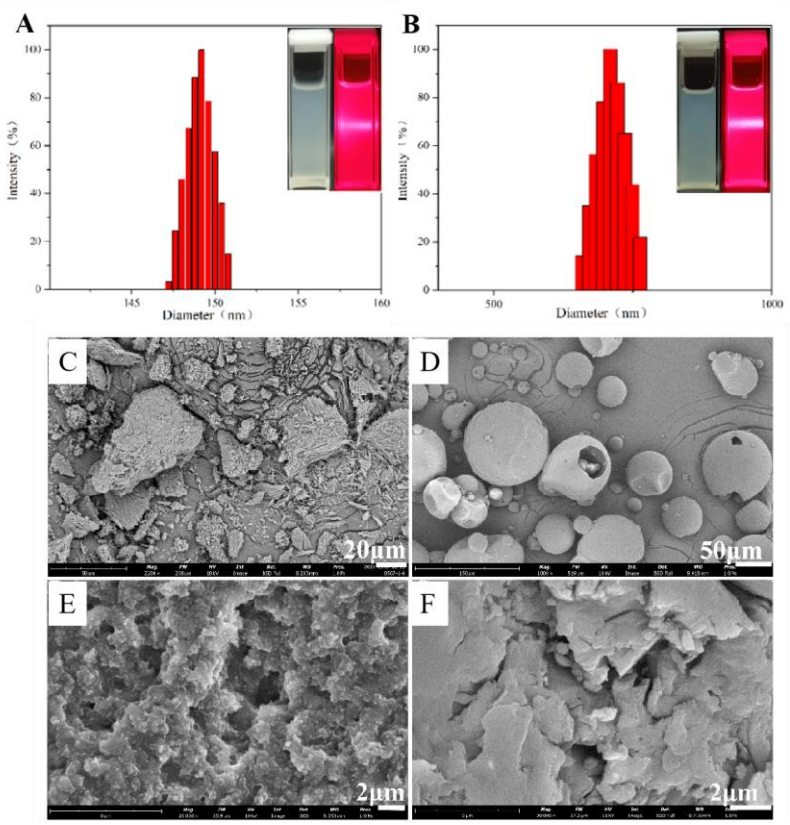

Figure 4. Particle size distribution and visual appearance of (A) freshly prepared SCU-PVP nanosuspension and (B) the corresponding nanoparticles; SEM images of (C) bulk SCU, (D) PVP, (E) nanosuspension, and (F) nanoparticles.

Figure 4. (**A**, **B**) shows that both freshly prepared and redispersed SCU-PVP nanosuspensions were translucent and exhibited a Tyndall effect, indicating the presence of colloidal systems. The average particle size was approximately 150 nm for the nanosuspensions and 700 nm for the dried nanoparticles, both with a relatively narrow size distributions (**Table S1**).

SEM images (**Figure 4. C- F**) revealed that bulk SCU appeared as large, irregularly aggregated, short fibrous crystals, whereas PVP exhibited hollow microspheres with diameters of of 20–100 μm. The SCU-PVP nanoparticles displayed a more uniform submicron structure, although larger aggregates formed during the drying process, consistent with the particle size data.

PVP acted as a stabilizer, adsorbing onto the surface of SCU colloidal particles and

preventing aggregation. Its hydrophilic nature and high viscosity slowed the sedimentation process, while also acting as a solid dispersion carrier to prevent excessive aggregation during drying.[27] This stabilization enabled the rapid redispersion of drug particles in aqueous media, enhancing the solubilization of SCU.

3.3 Differential Scanning Calorimetry (DSC) Analysis

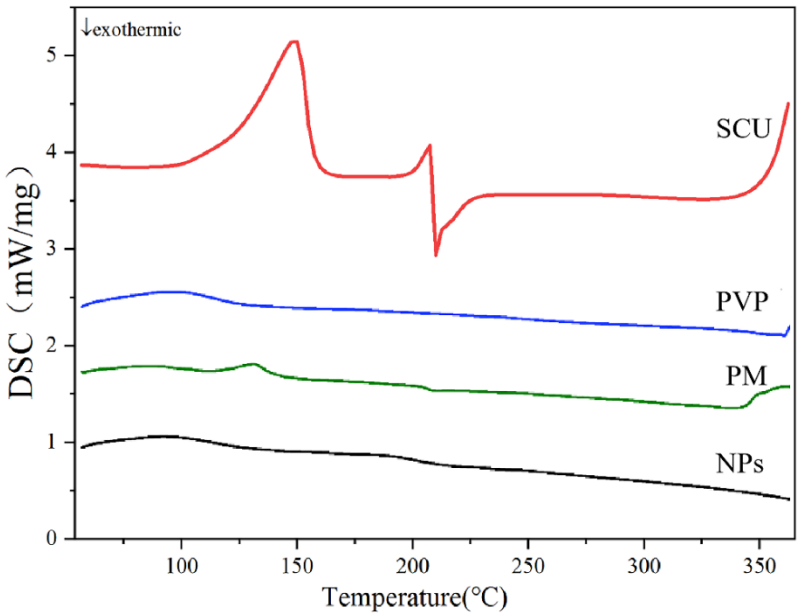

Figure 5. DSC thermograms of pure SCU, PVP K30, physical mixture (PM), and SCU nanoparticles (NPs).

The DSC thermograms (**Figure 5)** indicated that pure SCU exhibited an endothermic peak at 181.1°C and an exothermic peak at 210.3°C, consistent with its crystalline nature. In contrast, PVP K30, an amorphous polymer, showed no distinct peaks.[20] The physical mixture of SCU and PVP exhibited a slightly shifted endothermic peak attributed to SCU. However, the nanoparticle formulation did not display any sharp peaks, suggesting that the drug had transitioned into an amorphous state, which is beneficial for enhancing solubility and dissolution.

3.4 Powder X-Ray Diffraction (PXRD) Analysis

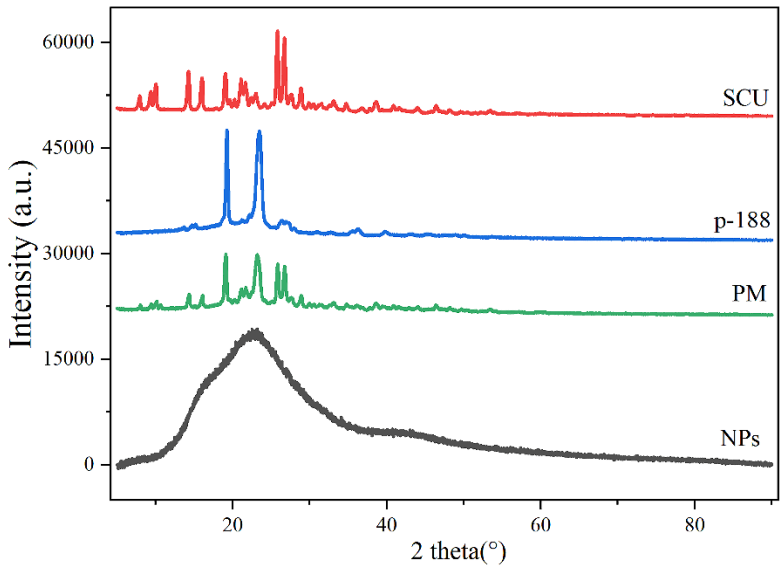

Figure 6. PXRD patterns of pure SCU, PVP K30, physical mixture, and SCU nanoparticles.

PXRD patterns (**Figure 6**) further confirmed the crystallinity of bulk SCU, as indicated by sharp peaks at specific 2θ angles . These peaks were also present in the physical mixture of SCU and PVP, indicating that SCU remained crystalline. However, the nanoparticle samples exhibited a broad peak with reduced intensity, confirming the successful transition of SCU to an amorphous form within the PVP matrix, which likely contributed to improved solubility and dissolution.

3.5 Fourier-Transform Infrared (FTIR) Analysis

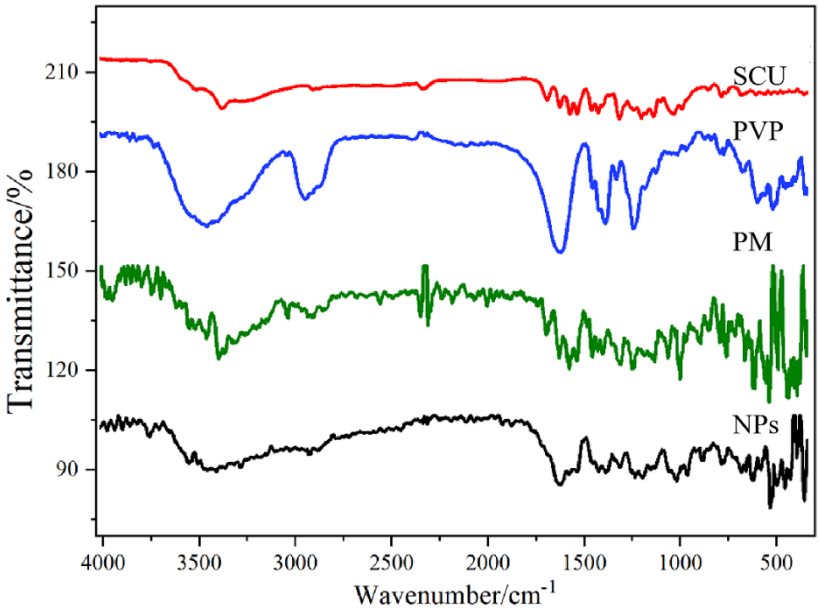

Figure 7. FTIR spectra of pure SCU, PVP K30, physical mixture, and SCU nanoparticles.

FTIR spectroscopy (**Figure 7**) was used to investigate the interactions between SCU and PVP. The characteristic peaks of SCU at 3509.6, 3373.8, and 3275.5 cm^{-1} (corresponding to –OH stretching) and 1720.9 cm^{-1} (C=O stretching) remained unchanged in the physical mixture, indicating no significant interaction between the components.[13,28] However, the FTIR spectrum of the SCU-PVP nanoparticles revealed shifts in these peaks, suggesting hydrogen bonding between the hydroxyl groups of SCU and the carbonyl groups of PVP. This bonding played a crucial role in the stabilization and amorphization of the nanoparticles.

3.6 Molecular Miscibility Calculation

Table 1. Calculated HSP parameters for SCU and PVP.

Parameters	SCU	PVP
δ_d , $MP_a^{0.5}$	20.4	17.9
δ_p , $MP_a^{0.5}$	8.3	8.4
δ_h , $MP_a^{0.5}$	15.3	6.3
δ_t , $MP_a^{0.5}$	26.8	20.8

δ_v , $MP_a^{0.5}$	22.0	19.8
$\Delta\delta_t$, $MP_a^{0.5}$	-	6.0
$\Delta\bar{\delta}$, $MP_a^{0.5}$	-	9.3
R_a , $MP_a^{0.5}$	-	10.3

Table 1 presents the calculated Hansen solubility parameters (HSP) for SCU and PVP. The data indicated that SCU and PVP were miscible, as the differences in Δδt, Δδ, and Ra were below the critical thresholds of 8.18, 16.87, and 17.64 $MP_a^{0.5}$, respectively.[29] These findings further support the formation of stable SCU-PVP nanoparticles.

3.7 Drug Content Determination

The DL and EE of SCU in the nanoparticles (**Figure 8A**) were favorable, exceeding 40% and 85%, respectively. This high efficiency can be attributed to the low solubility of SCU in DCM, which facilitated efficient drug precipitation, and to the protective colloidal action of PVP, which helped stabilize the nanoparticles and prevent drug loss during the preparation process.

3.8 Saturated Solubility of SCU

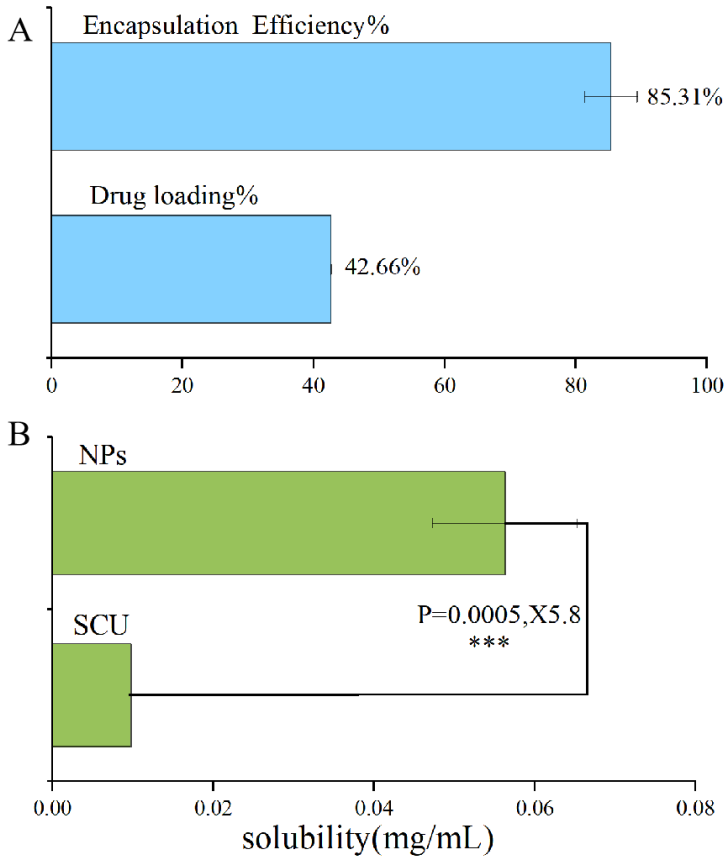

Figure 8. (A) Drug loading and encapsulation efficiency of SCU-loaded nanoparticles; (B) SCU solubility of pure drug and of drug nanoparticles in water. (mean ± SD, n=3)

In water, the SCU-PVP nanoparticles exhibited significantly higher solubility than pure SCU (**Figure 8B**), consistent with previous reports that PVP enhances the aqueous solubility of poorly soluble drugs by promoting hydrogen bonding and forming amorphous structures.

3.9 *In vitro* Dissolution Test

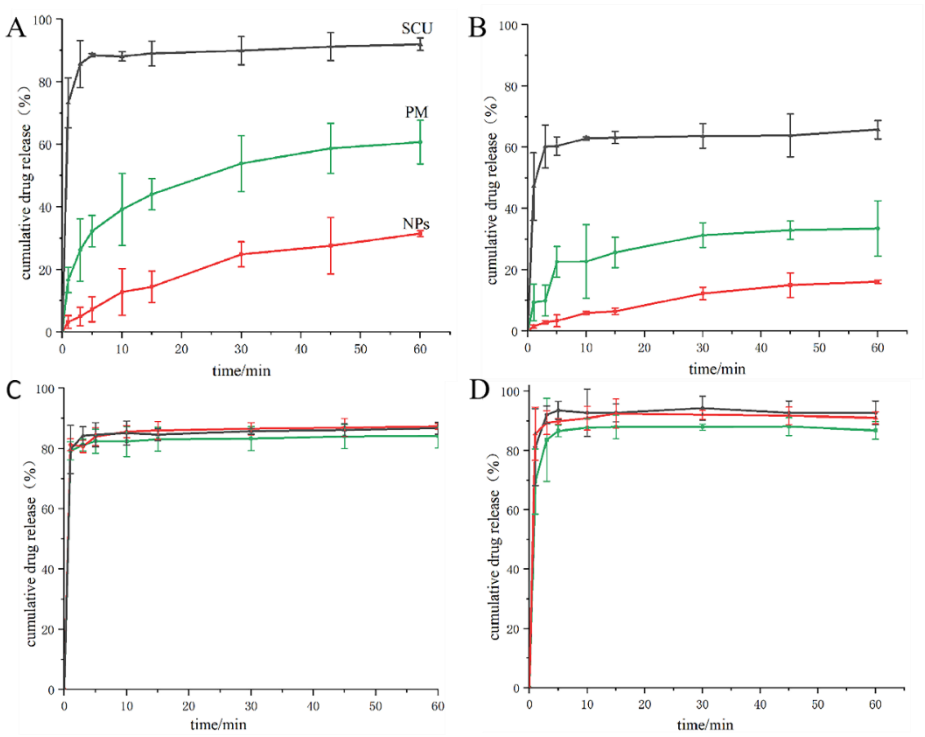

Figure 9. *In vitro* drug dissolution profiles of pure drug (red line), physical mixture (green line) and nanoparticles (black line) in purified water (A) or in PBS solutions at (B) pH 5.0; (C) pH 6.8; (D) pH 7.4.

The *in vitro* dissolution profiles of SCU nanoparticles, physical mixtures, and pure SCU in various media are shown in **Figure 9**. All SCU-PVP nanoparticle samples exhibited rapid drug release, with over 60% of SCU released within the first minute. In contrast, the physical mixtures released just over 20% within the first 5 minutes, while pure SCU released less than 3% over the same period, eventually reaching only about 17% after 60 minutes. The presence of PVP in the formulations significantly enhanced SCU dissolution, likely due to the increased solubility of SCU in PVP-containing aqueous solutions.

When pH 5.0 PBS was used as the dissolution medium, the SCU nanoparticles released approximately 70% of their drug content within the first 5 minutes and eventually reaching a plateau of nearly 90%. In comparison, the physical mixture and pure SCU powder released around 31% and 8% within the same timeframe, respectively, with gradual increases to 60% and 30% after 60 minutes. At pH values of 6.8 and 7.4, all samples showed over 80% SCU release within 5 minutes, indicating that SCU solubility is lower under acidic conditions than

under neutral or basic conditions.

The similarity factor (f_2) analysis (**Table S2**) revealed a pH-dependent dissolution behavior. In purified water and acidic medium (pH 5.0), the f_2 values (29 and 39, respectively) were significantly lower than 50, confirming the superior dissolution of NPs over PM. However, in neutral to basic media (pH 6.8 and 7.4), the f_2 values increased to 70 and 57, respectively, indicating similar dissolution profiles.[30]

These results suggest that the SCU-PVP nanoparticle formulation has the potential to significantly improve bioavailability following oral administration.

3.10 *In vivo* Oral Pharmacokinetic Study

The plasma concentration-time profiles of SCU in rats are shown in **Figure 10**, and the pharmacokinetic parameters are summarized in **Table 3**.

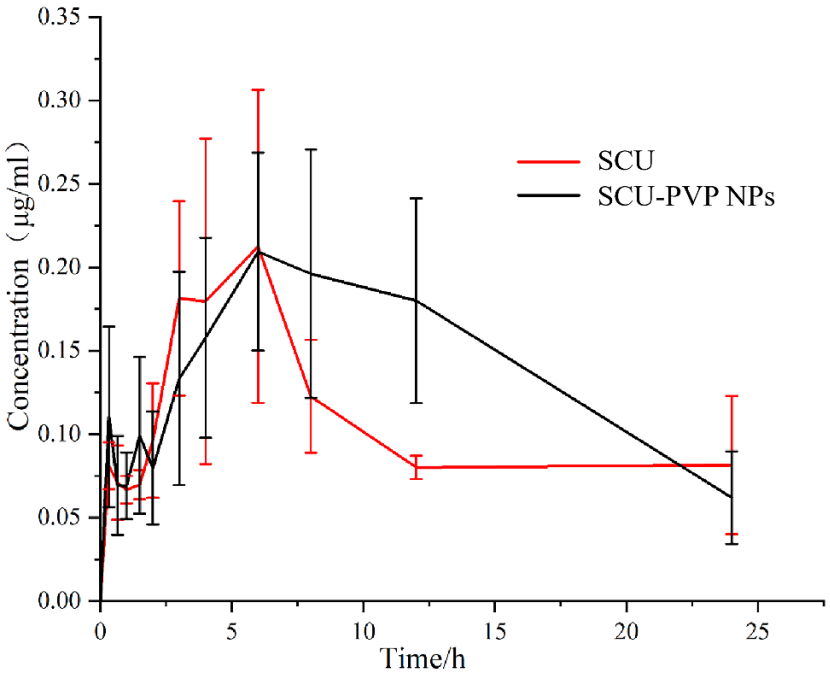

Figure 10. Plasma concentration-time curves of pure scutellarin and nanoparticles in SD rats following oral administration (mean ± S.D, n=6).

Table 2. Pharmacokinetic parameters of pure scutellarin and nanoparticles in SD rats after oral administration (mean ± S.D, n=6).

Parameters	SCU	nanoparticles
AUC_{0-t}, mg/L*h	2.58±0.536	3.386±0.904
$AUC_{0-\infty}$, mg/L*h	2.927±0.271	4.369±1.208*
T_{max}, h	4.667±1.506	6.065±2.971
C_{max}, mg/L	0.255±0.09	0.248±0.035
$t_{1/2}$, h	8.47±10.279	10.048±4.041
MRT_{0-t}, h	10.508±1.039	10.351±0.487
$MRT_{0-\infty}$, h	15.797±11.757	17.131±4.636
Cl, L/h/Kg	34.423±3.314	24.573±7.624

*$P<0.05$ versus the pure SCU group.

The SCU-PVP nanoparticle formulation resulted in higher AUC, T_{max}, and $T_{1/2}$ values compared with pure SCU, indicating improved absorption and prolonged systemic circulation. Although there were no significant differences in C_{max} and MRT_{0-t} between the groups, the nanoparticle formulation showed reduced plasma clearance, likely due to longer retention of SCU in circulation. Overall, the relative oral bioavailability of SCU-PVP nanoparticles was approximately 130% compared to pure SCU.

The SCU-PVP nanoparticles demonstrated significantly higher oral bioavailability compared to bulk SCU. The AUC of the SCU-PVP nanoparticles was approximately 1.3 times that of the bulk SCU, indicating a 130% relative bioavailability. This enhancement can be attributed to the improved solubility and dissolution rate of SCU in the amorphous nanoparticle form. The T_{max} for the nanoparticles was longer compared to the bulk SCU, suggesting a more sustained release profile. The elimination half-life ($T_{1/2}$) of SCU from the nanoparticles was also extended, indicating prolonged systemic circulation and slower clearance compared to the bulk SCU formulation.

Although the C_{max} values of the two groups were similar, the slower clearance and extended $T_{1/2}$ of the nanoparticle formulation suggest that SCU in nanoparticle form remained in the bloodstream for a longer duration, potentially enhancing its therapeutic efficacy. These findings highlight the advantages of the SCU-PVP nanoparticle formulation in improving oral

bioavailability, making it a promising approach for enhancing the pharmacokinetic performance of poorly soluble drugs like SCU.

4. Conclusion

In this study, we successfully developed amorphous SCU-PVP nanoparticles using a simple anti-solvent precipitation method assisted by ultrasonication. The nanoparticles were confirmed to be in an amorphous state, by DSC and PXRD analyses, while FTIR spectroscopy demonstrated hydrogen bonding between SCU and PVP. These nanoparticles exhibited improved dissolution rates in water and significantly enhanced oral bioavailability (130%) compared to pure SCU. This method of nanoparticle production offers a scalable and efficient approach to improving the solubility and bioavailability of poorly soluble drugs. Future studies will focus on formulation optimization, scaling up production, long-term stability assessment, and conducting *in vivo* toxicological and therapeutic evaluations to further explore the clinical potential of SCU-PVP nanoparticles.

Funding/Acknowledgement

This research was supported by the Applied Basic Research Joint Special Funds on Chinese Medicine of Yunnan Provincial Science and Technology Department (202001AZ070001-011, 202401AZ070001-106) and the Research Foundation of Education Bureau of Yunnan Province (2023J0550). This work was also partly supported by Reserve Talents Project for Young and Middle-Aged Academic and Technical Leaders of Yunnan Province (grant no. 202205AC160038).

CRediT authorship contribution statement

Xin Cheng: Formal analysis, Methodology, Writing – original draft.

Qin Lv: Formal analysis, Methodology, Writing – original draft.

Shuang Tian: Formal analysis, Methodology.

Guiyan Jin: Formal analysis, Methodology.

Wenbin Jin: Formal analysis, Methodology.

Jiao Wang: Formal analysis, Funding acquisition, Writing – original draft, review & editing.

Wenping Wang: Conceptualization, Funding acquisition, Writing – review & editing.

Competing Interests

The authors declare no conflict of interest.

Ethical Approval

All experimental procedures were carried out in consistent with the guideline of the Ethics committee of Yunnan University of Chinese Medicine (Approval code: YNUTCM-XMSS-G-20250014).

Data availability

Data will be made available on request.

Reference

1. Rathod NB, Elabed N, Punia S, Ozogul F, Kim SK, Rocha JM, et al. Recent developments in polyphenol applications on human health: a review with current knowledge. Plants. 2023;12(22):3869. doi:10.3390/plants12223869
2. Sun W, Shahrajabian MH. Therapeutic potential of phenolic compounds in medicinal plants—natural health products for human health. Molecules. 2023;28(4):1845. doi:10.3390/molecules28041845
3. Dwivedi K, Mandal AK, Afzal O, Altamimi AS, Sahoo A, Alossaimi MA, et al. Emergence of nano-based formulations for effective delivery of flavonoids against topical infectious disorders. Gels. 2023;9(7):545. doi:10.3390/gels9070545
4. Attar ES, Chaudhari VH, Deokar CG, Dyawanapelly S, Devarajan PV. Nano drug delivery strategies for an oral bioenhanced quercetin formulation. Eur J Drug Metab Pharmacokinet. 2023;48(5):495-514. doi:10.1007/s13318-023-00860-6
5. Prasad RD, Sarvalkar PD, Prasad N, Prasad RS, Prasad RB, Prasad RR, et al. Emerging trends of bioactive nano-materials in modern veterinary science and animal husbandry. ES Food Agrofor. 2024;18:1-15. doi:10.30919/esfaf1114
6. Fujii S. Polymeric core-crosslinked particles prepared via a nanoemulsion-mediated

process: from particle design and structural characterization to in vivo behavior in chemotherapy. Polym J. 2023;55(9):921-33. doi:10.1038/s41428-023-00812-2

7. Zhang H, Zhou Y, Xu C, Qin X, Guo Z, Wei H, et al. Mediation of synergistic chemotherapy and gene therapy via nanoparticles based on chitosan and ionic polysaccharides. Int J Biol Macromol. 2022;223:290-306. doi:10.1016/j.ijbiomac.2022.10.212
8. Gu S, Zhou Z, Zhang S, Cai Y. Advances in anti-diabetic cognitive dysfunction effect of Erigeron breviscapus (Vaniot) Hand-Mazz. Pharmaceuticals. 2022;15(12):1589. doi:10.3390/ph15121589
9. Vesaghhamedani S, Kiapey SS, Shabgah AG, Amiresmaili S, Jahanara A, Oveisee M, et al. From traditional medicine to modern oncology: Scutellarin, a promising natural compound in cancer treatment. Prog Biophys Mol Biol. 2023;180-181:19-27. doi:10.1016/j.pbiomolbio.2023.04.002
10. Dong X, Qu S. Erigeron breviscapus (Vant.) Hand-Mazz.: a promising natural neuroprotective agent for Alzheimer's disease. Front Pharmacol. 2022;13:858745. doi:10.3389/fphar.2022.858745
11. Zhang T, Li X, Xu J, Shao J, Ding M, Shi S. Preparation, characterization, and evaluation of breviscapine nanosuspension and its freeze-dried powder. Pharmaceutics. 2022;14(5):991. doi:10.3390/pharmaceutics14050991
12. Ma Y, Li H, Guan S. Enhancement of the oral bioavailability of breviscapine by nanoemulsions drug delivery system. Drug Dev Ind Pharm. 2015;41(2):177-82. doi:10.3109/03639045.2014.882934
13. Song Z, Yin J, Xiao P, Chen J, Gou J, Wang Y, et al. Improving breviscapine oral bioavailability by preparing nanosuspensions, liposomes and phospholipid complexes. Pharmaceutics. 2021;13(3):409. doi:10.3390/pharmaceutics13030409
14. Yang C, Zhao Q, Yang S, Wang L, Xu X, Li L, et al. Intravenous administration of scutellarin nanoparticles augments the protective effect against cerebral ischemia–reperfusion injury in rats. Mol Pharm. 2022;19(5):1410-21. doi:10.1021/acs.molpharmaceut.1c00844
15. Yang G, Li Z, Wu F, Chen M, Wang R, Zhu H, et al. Improving solubility and bioavailability of breviscapine with mesoporous silica nanoparticles prepared using ultrasound-assisted solution-enhanced dispersion by supercritical fluids method. Int J Nanomedicine. 2020;15:1661-75. doi:10.2147/IJN.S240600
16. Zhao K, Guo T, Wang C, Zhou Y, Xiong T, Wu L, et al. Glycoside scutellarin enhanced CD-MOF anchoring for laryngeal delivery. Acta Pharm Sin B. 2020;10(9):1709-18. doi:10.1016/j.apsb.2020.04.006
17. Waleka E, Stojek Z, Karbarz M. Activity of povidone in recent biomedical applications

with emphasis on micro- and nano drug delivery systems. Pharmaceutics. 2021;13(5):654. doi:10.3390/pharmaceutics13050654

18. Luo Y, Hong Y, Shen L, Wu F, Lin X. Multifunctional role of polyvinylpyrrolidone in pharmaceutical formulations. AAPS PharmSciTech. 2021;22(8):247. doi:10.1208/s12249-021-02148-2
19. Odeh AB, El-Sayed B, Knopp MM, Rades T, Blaabjerg LI. Influence of polyvinylpyrrolidone molecular weight and concentration on the precipitation inhibition of supersaturated solutions of poorly soluble drugs. Pharmaceutics. 2023;15(6):1695. doi:10.3390/pharmaceutics15061695
20. Koromili M, Kapourani A, Barmpalexis P. Preparation and evaluation of amorphous solid dispersions for enhancing luteolin's solubility in simulated saliva. Polymers (Basel). 2022;15(1):135. doi:10.3390/polym15010135
21. Cong W, Shen L, Xu D, Zhao L, Ruan K, Feng Y. Solid dispersion tablets of breviscapine with polyvinylpyrrolidone K30 for improved dissolution and bioavailability to commercial breviscapine tablets in beagle dogs. Eur J Drug Metab Pharmacokinet. 2014;39(3):203-10. doi:10.1007/s13318-013-0162-1
22. Zhang X, Guo T, Liu X, Kuang W, Zhong Y, Zhang M, et al. Anti-solvent precipitation for the preparation of nobiletin nano-particles under ultrasonication-cis/reverse homogenization. Ultrason Sonochem. 2023;96:106389. doi:10.1016/j.ultsonch.2023.106389
23. Yan T, Wang H, Song X, Yan T, Ding Y, Luo K, et al. Fabrication of apigenin nanoparticles using antisolvent crystallization technology: a comparison of supercritical antisolvent, ultrasonic-assisted liquid antisolvent, and high-pressure homogenization technologies. Int J Pharm. 2022;624:121981. doi:10.1016/j.ijpharm.2022.121981
24. Mohammad MA, Alhalaweh A, Velaga SP. Hansen solubility parameter as a tool to predict cocrystal formation. Int J Pharm. 2011;407(1-2):63-71. doi:10.1016/j.ijpharm.2011.01.028
25. AlBathish M, Gazy A, Jamal MA. A comparative pH-dissolution profile analysis of selected commercial levothyroxine formulations in Lebanon using anion-exchange HPLC method: implication on interchangeability. Adv Pharmacol Pharm Sci. 2025;2025:1-12. doi:10.1155/2025/4291625
26. Ma Y, Wang J, Dong Z, Yang Z, Cao T, Ma Y, et al. A novel organogel of breviscapine via supramolecular self-assembly in DCM. J Mol Liq. 2024;397:123917. doi:10.1016/j.molliq.2024.123917
27. Kurakula M, Rao GSNK. Pharmaceutical assessment of polyvinylpyrrolidone (PVP): as excipient from conventional to controlled delivery systems with a spotlight on COVID-19 inhibition. J Drug Deliv Sci Technol. 2020;60:102046.

doi:10.1016/j.jddst.2020.102046

28. Febriyenti F, Indra P, Zaini E, Ismed F, Lucida H. Preparation and characterization of quercetin-polyvinylpyrrolidone K-30 spray dried solid dispersion. J Pharm Pharmacogn Res. 2020;8(2):127-34. doi:10.56499/jppres19.714_8.2.127
29. Salem A, Nagy S, Pál S, Széchenyi A. Reliability of the Hansen solubility parameters as co-crystal formation prediction tool. Int J Pharm. 2019;558:319-27. doi:10.1016/j.ijpharm.2019.01.015
30. Xu Z, Cuquerella-Gilabert M, Zarzoso-Foj J, Merino-Sanjuan M, Mangas-Sanjuan V, García-Arieta A. Comparison of dissolution profiles: 90% confidence intervals of different f2 estimators using bootstrap methodology versus the Euclidean Distance of the Non-standardized Expected (EDNE) values. Eur J Pharm Biopharm. 2025;216:114839. doi:10.1016/j.ejpb.2025.114839